Preparation and characterization of novel eggshell membrane-chitosan blend films for potential wound-care dressing: From waste to medicinal products

Xiaoyun Li[1], Meihu Ma[1], Dong Uk Ahn[2], Xi Huang[1]*

[1]*College of Food Science and Technology, National Research and Development Centre for Egg Processing, Huazhong Agricultural University, No 1 Shizishan Street, Wuhan, 430070, P.R. China;* [2]Department of Animal Science, Iowa State University, Ames, IA 50011, USA

Abstract: A series of different eggshell membrane (ESM) and chitosan (CS) blend films (ESM/CS) were prepared for wound-care dressing. The appearance, transparency and microstructure of the films were characterized. Several wound care-related properties such as the film integrity in solution, pH, protein (BSA) and wound fluid absorption capacity as well as the antibacterial property of ESM/CS films were evaluated. The blend films were more stable than CS film after 95 hours of incubation in solution. The integrity of the blend films improved significantly at the cost of a small insignificant decrease in wound fluid absorption capacity. Besides, the blend films provided an acidic environment (pH = 5.86) for wound healing. The swelling properties of ESM contributed significantly to the increase of BSA absorption capacity of the blend films (from 46.57 mg/g of CS film to 61.07 mg/g of blend film) and helped absorb more nutrients to promote the proliferation and migration of fibroblasts. Addition of CS to ESM also enhanced the antibacterial activity of the films significantly. The results indicated that the EMS/CS blend films with 0.01 g ESM/mL CS solution showed the highest high potential to be used as a wound-care dressing for humans as well as animals.

Keywords: wound healing; eggshell membrane; antibacterial activity

1. Introduction

There are a large number of patients suffering from various destructive types of cutaneous wounds caused by trauma, burns, or other conditions such as sickle cell anemia leg ulcer in China [1]. Wound-healing is a multifaceted complex and dynamic biological processes such as inflammation, cell proliferation and tissue remodeling, and having a high nutrient exchange capacity and an acidic microenvironment is essential for cell proliferation and self-healing process, respectively [3, 4]. A suitable wound-care dressing can promote the wound healing process by maintaining

* Corresponding author, Tel.: +86 027 87283177. E-mail address: huangxi@mail.hzau.edu.cn

moderate humility of the wound area, helping exchange of nutrients, and keeping the area from microbial infection. Thus, the wound-care dressings should have high biocompatibility, antimicrobial activity, liquid absorptivity, and modest physical and mechanical strength.

Nowadays, various natural polymers with strong antibacterial properties, effective hemostasis or scar-repairing ability have been developed as wound-care dressing materials. Among them, chitosan (CS), a positively-charged polysaccharide containing glucosamine, is considered as a cheap, safe and effective natural material for wound-care dressings [5, 6]. Because CS has various prominent biomedical properties, including biocompatibility, film-forming ability, broad antimicrobial activity, high hemostatic capacity, and excellent adhering ability to injured tissues and vessels to seal off the wounds [7, 8]. Nonetheless, using CS as a wound-care dressing is still limited because of its poor mechanical strength in acidic solutions [8]. According to our preliminary experiments where the CS films were immersed in the exudate of the wounds, it was easily dissolved because of its molecular structure with a large number of hydroxyl groups. Thus, CS films are not conducive to use for the long-term healing of wounds. Various crosslinking strategies (i.e., glutaraldehyde or transglutaminase) have been studied to enhance the mechanical and water-resistance properties of CS films. However, the cross-linking agents may be cytotoxic and have adverse effects on human health. Furthermore, it is difficult for a single polymer or biomaterial to meet all the general requirements for a perfect wound-care dressing. Therefore, CS has been blended with other macromolecular polymers or biomaterials such as cellulose acetate [9], lysozyme [10], bentonite [8] and silk fibroin [11] to enhance its functionalities as a wound-care dressing material. To the best of our knowledge, no research work on producing wound-care dressing materials by blending CS and eggshell membrane has been conducted.

About 5 million tons of eggshells are produced as a by-product of 10^{12} eggs annually in the world and are generally overlooked and disposed as the industrial and household wastes [12]. Eggshell membrane (ESM), a complex mixture of proteins (i.e., kept in and collagen) and glycoprotein (i.e., hyaluronic acid, glucosamine), has been proposed as a highly-value material for biological and biomedical engineering because of its nontoxic, protein-rich and biocompatible characteristics [1, 13]. ESM named "Phoenix cloth" has been used as a medicinal ingredient for healing burn, corneal ulcer, and decubitus ulcer in Chinese traditional medicine for more than 400 years. Sumo wrestlers still use it as a first aid wound-care dressing in Japan [14, 15]. Levytska et al. found that ESM could be considered as a skin-graft donor site dressing due to its pain relief, wound protection and healing acceleration properties [16]. Yang et al. showed that ESM could effectively promote the quick epithelialization of split-thickness skin graft donor sites and reduce subjective pain sensations [17]. To assess the practicability of ESM as a home remedy for lacerations and abrasions, some scholars used it on a rat model to help wound-healing. The results showed that ESM could be incorporated into bandages [18]. Also, it can be applied to the existing CS film as a remedy to improve its poor mechanical strength.

The main objective of this study was to prepare functional blend films using CS

and ESM (ESM/CS) and compare their physical and biological properties such as thickness, appearance, surface morphology, and pH, wound fluid absorption capacity, BSA absorption capacity, degradation ability, and antibacterial activity. The prepared films were also evaluated for their potential applications as a biomaterial for wound-care dressing.

2. Materials and methods

2.1. Materials

Chitosan (CS) with the molecular weight of 100,000 and with 80%~95% deacetylation was obtained as a gift from Sinopharm Chemical Reagent Co., Ltd. Glycerol (G) was purchased from Sinopharm Chemical Reagent Co. Ltd. Eggshell membrane (ESM) was purchased from Heilongjiang Xinghe Agriculture Co., Ltd. Bovine serum albumin, acetic acid, and other chemicals were received from Sinopharm Chemical Reagent Co., Ltd and used without further purification.

2.2. Particle Size Detection of ESM powder

The average particle size distribution of ESM powder was measured using APA2000 laser particle size distribution instrument (Malvern, UK).

2.3. Preparation of ESM/CS films

One gram of CS powder was dispersed in 100 mL of 1% (v/v) acetic acid solution and continuously stirred at 50 ^{o}C until a clear solution is obtained. The ESM powder was added to 10 mL of CS solution to obtain 0.01 g, 0.02 g or 0.03 g ESM per mL CS solution. The solutions were stirred continually using a magnetic stir until the ESM powder was dispersed entirely, and then glycerol (0%, 1% or 2%, v/v) was added to the CS/ESM suspensions to form homogeneous casting solutions. Finally, the suspension was cast on a 12-well plate and dried at 37 ^{o}C to form ESM/CS films. The CS film (control) was prepared using the same procedure without ESM powder. According to the amount of glycerol (G) and ESM powder, the blend membrane was named xG-yESM/CS film (Table 1; x=0, 1, 2, the volume ratio of glycerol; y=0, 0.01, 0.02, 0.03, the mass ratio of ESM).

2.4. Morphological characterization of ESM/CS films

The visual assessments were made using the appearance, thickness, mass uniformity, transparency and microscopic morphology of the ESM/CS films. The thickness of films was measured with an electronic digital micrometer at three different positions of one film. The transparency was measured by placing the films on a printed paper with green patterns. The mass uniformity of the films prepared were measured using two methods: for the uniformity of the films from casting plates was assessed by making a circular cut (10 mm in diameter) from a film and individually weighing the cut-film, and the uniformity of each individual film was determined by making three small circular cuts (5 mm in diameter) from a film and comparing the weight of the cut-films. The micromorphology of films was observed

using a scanning electron microscopy (SEM) (JSM-6390LV, Japan) operated at 10 kV accelerating voltage.

2.5. Evaluation of integrity of ESM/CS films and degradation in vitro

The integrity and degradation of ESM/CS films in vitro were measured using the method described by Ma et al. [19, 20]. The prepared films (12×12 mm) with a known weight were immersed into 1 mg/mL lysozyme/PBS at 37□ for 1 hr (D_i) to swell and equilibrate before use. The equilibrated films were removed, washed with distilled water, wiped off the residual water, and weighed (D_t). The pre-equilibrated films were further immersed in 1 mg/mL lysozyme/PBS at 37□ for 1, 2, 3, 4, 23, 47, 71 and 95 h, and weighed at the designated time (D_t). The relative degradation ratio (RDR) was calculated using the following equation:

$$RDR\ (\%) = (D_i - D_t)/D_i \times 100$$

where

D_i is the initial weight after 1 hr equilibration

D_t is the weight after t-hours of incubation (t = 1, 2, 3, 4, 23, 47, 71, 95).

2.6. Wound healing ability of ESM/CS films in vitro

2.6.1 Microenvironmental pH of ESM/CS films

The films were cut into pieces (12×12 mm) and then immersed in 4 mL of normal saline solution (0.9%) for 24 h at 25□. The pH of the soaking solution was determined to evaluate the microenvironment created by the films [8].

2.6.2 Wound fluid absorption capacity of the blend films

The wound liquid absorptivity of the films was estimated using the simulated wound fluid (SWF) [21]. The weighed films (I_0) were immersed into SWF consisting of 2% w/v of BSA solution, 0.08 M tris methylamine, 0.4 M NaCl, and 0.02 M $CaCl_2$ in distilled water (pH=7.5). At predetermined time points, the weight of the swollen films (I_s) was measured after the excess SWF on the surface was removed by blotting with a filter paper. The wound fluid absorption rate (WFA) was calculated using the following equation.

$$WFA\ (\%) = \frac{I_s}{I_0} \times 100$$

2.6.3 BSA absorption capacity of the blend films

The BSA absorption capacity of the films was estimated according to Cao's method [22]. In brief, about 30 mg of film fragments were placed in a 24-well cell culture plate. After equilibrated with PBS buffer for 2-3 h, all the samples in triplicate were incubated with 0.75 mL of 10 mg/L BSA solution for 24 h at 37 ^{o}C. The absorbed amount of BSA was calculated using the concentration change of BSA

solutions before and after incubation. The group without any film was treated as the control. The BSA concentration was measured using a bicinchoninic acid (BCA) protein assay kit (Servicebio, China).

2.7. Antibacterial assessment

To detect the antibacterial performance of the blend films, a bacterial suspension assay was conducted using the process developed by Li et al. with some modifications [23, 24]. In brief, the films with a diameter of 22 mm were sterilized by dipping in 75% ethanol for 30 min and washed with PBS for three times in super-clean worktable, and then excess moisture on the surface of films was blown dry in the case of sterile air convection while all the conditions were kept sterile. One mL of a bacterial stock was inoculated for 8-12 h in 10 mL Trypticase soy broth (TSB) medium with a constant shake at 180 rpm at 37 ^{o}C. The fresh *Escherichia coli* (devoted as *E. coli*) and *Staphylococcus aureus* (devoted as *S. aureus*) strains were diluted separately in normal saline to obtain an O.D (optical density) reading of 0.07 at 595 nm. Then, 1.5 mL of the diluted bacterial solution and 1.5 mL TSB medium were mixed, and the blended solution (in total 3 mL) was dispensed into the wells of 12-well plate containing the films. The plates containing bacteria solution were cultivated for 24 h with a gentle shake at 50 rpm at 37 ^{o}C. 200 μL of the bacterial solution was transferred into a 96-well culture plate, and the O.D reading was recorded with the Microplate reader (Biotek, USA). The assay was performed in triplicates.

3. Results

3.1. The size distribution of ESM powder

As shown in Fig. 1, the particle sizes distribution of ESM was in a range between 10.01 μm to 316.22 μm, and the average diameter of ESM powder was 117.25 μm, which provided sufficient support for uniformity of the films (Table. 2). As discussed above, the commercial ESM powder without any treatment was a kind of micronized particles, which was different from the nanoparticles used to prepare a dressing of wound healing [25, 26]. Matthews et al. successfully prepared the lyophilized wound healing wafers, which were composed of metalloproteinase-3 and stromelysin-1 inhibitor with the mean particle size of about 878.7 μm [27]. Zheng et al. adopted the micronized amnion (300-600 μm) to treat wounds in diabetic mice [28]. Other wound-healing dressings based on ESM have been developed recently, and the dressings mainly used the ESM as a biotemplate [24] or adsorbent [1], but not for its function on wound healing.

3.2. Morphological characterization of ESM/CS films

There are many general requirements for a kind of wound healing dressing, such as flexibility, tearability, integrity, transparency, and uniformity. However, due to the hydrophobicity and hardness of ESM, the blend films would also be hard and have poor flexibility and low mechanical strength. Several previous research demonstrated

that addition of glycerol, a plasticizer, in CS matrixes not only increased the flexibility of films but also improved their mechanical properties [29, 30]. Hence, a certain amount of glycerol was added to increase the flexibility and controllability of the films. The appearance (Fig. 2A) and transparency (Fig. 2B) of the CS and blend films with varying ratios of glycerol and ESM powder are shown in Figure. 2. The green patterns on the background could be identified clearly through CS films and some blend films. The CS film was transparent without any color tint, but the blend films showed yellowish-brown tint after adding ESM powder, which was attributed to the yellowness of ESM powder. The xG-ESM/CS (x=1%, 2%, and y=0.01, 0.02) films could be uncovered easily in the process of experiment, but the films with excess ESM powder (y=0.03 g/mL) as well as those without any glycerol (x=0) were too hard to be detached from the container surface. Therefore, the films containing 0.03 g/mL ESM powder or that without any glycerol were inappropriate. What is noteworthy is that the appearance and homogeneity of the films with the 0.01 g/mL of ESM powder are similar to those of the CS/bentonite nanocomposite films and the CS-based films prepared through a casting/solvent evaporation method in references [8, 20]. Addition of glycerol had no effect on the transparency of the cast films, which agree with the previous reports [30].

Uniformity is a major parameter that indicates a correct preparation method for a blend film [31]. The thickness of all films was in the range of 0.17 ± 0.07 μm to 0.24 ± 0.03 μm, and there were no significant variations in the thickness of all blend films (Table 2). The mass of prepared films was dependent on the content of ESM powder. The films with 0.01 g/mL ESM powder were lighter than 0.02 g/mL ones (Table. 2), which might be due to the enhanced density of ESM films with the increased content of undissolved ESM powder. The influence of glycerol to the thickness of films was negligible, indicating that the method for preparation of xG-yESM/CS film was consistent.

The SEM analysis of films was presented in Fig. 3. The surface of CS films (Fig. 3a) was flat, smooth and compact without any cracks or particles on the surface, while rough and wrinkly surfaces were found in the blend films (Fig. 3b-e) due to the added ESM in CS solution. The degree of roughness on the surface of blend films increased as the amount of ESM powder added increased. The rough surface in wound dressing also was observed in CS/bentonite blend films prepared by Nouri et al. [32].

3.3. Evaluation of integrity of ESM/CS films and degradation in vitro

The relative degradation ratio (RDR) of CS and blend films are summarized in Fig. 4. After soaking in lysozyme/PBS solution for 95 hours, the RDR of CS film was 66.10% with over half of the weight degraded, while that of the 1G-0.01 ESM/CS, 2G-0.01 ESM/CS, 1G-0.02 ESM/CS film and 2G-0.02 ESM/CS film were 33.25%, 28.08%, 27.07%, and 35.51%, respectively. So, the blend films presented lower degradation degree than the CS film after 95-hour incubation. The blend films could be considered as an acceptable wound-care dressing with low degradation rate in particular in 2G-0.01ESM/CS and 1G-0.02ESM/CS films. The photographs of CS and

blend films immersed in PBS at different time (1 day, 2 days and 3 days) are exhibited in Fig. 4a. As opposed to the gradual curling and dissolution of CS film, all blend films maintained their integrity except for 1G-0.01 ESM/CS that showed curly external appearance due to the high content of CS and low glycerol in the film.

Because of its low toxicity, hemostatic potential, good film-forming properties, and anti-microbial activity, CS-based films gained considerable attention for wound healing applications [33, 34]. Even so, the integrity of CS film was easily destroyed when it was soaked in normal saline or wound fluid. The CS can be dissolved easily in acidic solution, which restricted its application as a commercial wound-care dressing material. Therefore, it is essential to enhance the integrity of CS film in solution and prevent its degradation [20, 22]. The improvement of mechanical strength in ESM/CS blend films is related to the reinforced network structures by calcium as a cross-linker and physical filling [35, 36].

ESM is composed of a double membrane, in which the outer membrane adheres to the eggshell and plays a role in eggshell mineralization [22]. Calcium is found in the outer layer of ESM [37], and the calcium ions can be released from the outer ESM layer to an acidic casting solution. The network structure was reinforced by the electrostatic attraction between CS and calcium ions, enhancing the integrity of blend films in solution [38]. Also, calcium ions are involved in stanching, induction of platelets adherence, promotion of blood clotting and creation of anti-inflammatory cytokines. So, it is feasible and more conducive for the healing of wounds by introducing calcium ions [39, 40]. ESM powder may also act as a physical filler in the process of film-forming of CS and help keep the integrity of films. The glycerol added into the blend films is a widely-used polymer additive and have a positive effect on the flexibility and mechanical properties of CS films [41]. The improved flexibility and high mechanical endurance of the would-care dressing materials not only can endow it with a lasting function until the wound is completely healed, but also can contribute to be an appropriate substrate for adhesion, proliferation and migrations of cells [42,43].

3.4. Wound healing ability of ESM/CS films in vitro

3.4.1 Microenvironmental pH of ESM/CS films

Favorable external microenvironment for wound healing of our skin can be produced by modifying some parameters such as pH, temperature, and partial pressure of carbon dioxide or oxygen. A suitable microenvironmental pH might indirectly alter the internal microenvironment of the wound by inducing proliferation of fibroblasts [44]. Therefore, the pH of a good wound dressing should be similar to that of the normal healthy skin that ranges between 4.0 and 6.8. Fig. 5 showed that all the ESM/CS blend films exhibited a weakly acidic pH (between 5.86 and 6.52), which agreed with the pH values of commercially available wound-care products reported by other researchers. This also indicated that the blend films prepared in this study could act as an acidic medium to minimize the invasion of bacteria and stimulate the proliferation of fibroblasts indirectly during the wound-healing process [45].

3.4.2 Wound fluid and BSA absorption capacity

The wound fluid absorption rates (WFA) of the films in the simulated wound fluid (SWF) are presented in Fig. 6A. Compared with CS film (1276.01%), blend films showed lower WFA (90.43%~235.04%), which is attributed to hydrophobic properties of ESM added in the blend films [24]. This suggested that the integrity of blend films in solution increased with only a slight sacrifice of wound fluid absorption (Fig. 4a and 6A). Fig. 6A also showed the effect of ESM and glycerol on wound fluid absorption of blend films. The WFA increased from 102.23% (0G-0.01ESM/CS) to 112.34% and 228.6%, when 1% and 2% glycerol were added, respectively. It has been reported that wound fluid is absorbed into the films by two processes: water was bound to the material itself and retained in the pore space of the membrane [20]. However, there is no pore structure in the dense films as shown in SEM images (Fig. 3b-e). Therefore, when the concentration of ESM was 0.01 g/mL, the addition of glycerol improved the absorption of wound fluid because of abundant -OH groups in glycerol [46]. However, when 0.02g/mL of ESM was added, the wound fluid absorption of blend films was negatively correlated with the content of glycerol probably due to the reduction of hydrophilic material on the film surface. Although, the concentration of glycerol rose from 1% to 2%, the effect of hydrophobicity of ESM powder was greater than the effect of the hydrophilic action of glycerol, leading to lower absorption of wound fluid.

In addition to the wound fluid absorption, protein absorption of the dressing materials is also an important factor for wound healing. Bovine serum albumin (BSA), a protein similar to human serum albumin (HSA), is deemed an essential protein in the body that regulates osmotic pressure and transportation and is a nutrient [47, 48]. Therefore, BSA was used as a model protein to detect the protein absorption capacity of films in this study. It is known that films with high protein absorption can hold sufficient nutrients for cell proliferation and migration, facilitating wound healing [49]. In general, the absorption process of BSA is involved with the migration of water and BSA. There could be some difference in migration speed between water and BSA because the molecular mass of BSA is bigger than water.

As shown in Fig. 6B, CS and the blend films containing 0.01 g/mL of ESM powder exhibited a certain level of BSA absorption capacity. Compared to the absorption capacity of 46.57 mg/g of CS film, the BSA absorption capacity of blend films with 0.01 g/mL ESM (61.07 mg/g) was higher than that of the CS film. The swelling ratio of CS film was significantly higher than that of the blend films (Fig. 6A). During this process, water molecules permeated through the CS films more efficiently than the BSA macromolecule, which caused the CS film hyper-saturated, limiting to the absorption of BSA. So, the films with a lower ratio of swelling (1G-0.02ESM/CS and 2G-0.02ESM/CS film) absorbed more BSA than CS film. When the amount of ESM in films increased further to 0.02 g/mL, the BSA absorption of blend films decreased to 25.60 mg/g (1G-0.02ESM/CS) and 20.09 mg/g (2G-0.02ESM/CS), respectively. In this case, the migration of water and BSA were both restricted due to the hydrophobic property of ESM powder, causing lower BSA

absorption capacity. Thus, 1G-0.01ESM/CS and 2G-0.01ESM/CS can hold more nutrients to promote the proliferation and migration of fibroblasts and accelerate the rate of wound healing significantly.

3.5. Antibacterial assessment

An ideal dressing for skin regeneration should have adequate antibacterial activity, effectively protecting the injury from bacterial infection and providing a favorable environment for the growth of tissues [24]. Therefore, the antibacterial study is indispensable to investigate the efficacy of dressing materials for wound healing applications. The antimicrobial activities of CS and blend films were evaluated against two different bacterial strains, namely gram-negative *Escherichia coli*, gram-positive *Staphylococcus aureus*, using the suspension culture method (measurement of OD after treatment). As shown in Fig. 7, control sample incubated with *Escherichia coli* (Fig. 7A) and *Staphylococcus aureus* (Fig. 7B) without any film showed an increased OD value, from 0.07 to 0.98 after 24 h of incubation. For both of the bacterial strains, the final OD values (after 24 h of incubation) of CS and blend films were lower than those of the control samples. Among them, the OD value of 2G-0.01ESM/CS of *Staphylococcus aureus* (Fig. 7B) and *Escherichia coli* (Fig. 7A) were 0.42 and 0.27, respectively, which showed the highest antibacterial activity against those bacteria among the films. This improvement was attributed to the intrinsic antimicrobial activities of CS and the residual ovotransferrin and lysozyme in ESM [24, 36]. These results indicate that 2G-0.01ESM/CS is the best blend of film conditions for biomedical applications as a wound dressing.

4. Conclusions

A new type of CS and ESM blend films named xG-yESM/CS have been prepared using the film-casting method for wound-care dressing. The properties such as water resistance, wound fluid absorption, BSA absorption capacity and antibacterial activity that are related to wound healing were improved with the incorporation of 0.01 g/mL ESM and 2% glycerol into chitosan film (2G-0.01ESM/CS). This blend film (2G-0.01ESM/CS) can have a potential to be a material for wound-care dressing and the cell and animal experiments are in progress.

Conflict of interest

None.

Acknowledgments

This work was supported by the National Key Research and Development Program of China (2018YFD0400302) and General Program of National Natural Science Foundation of China (31471602).

Reference

[1] M Liu, G Luo, Y Wang, R Xu, Y Wang, WF He, JL Tan, M Xing, J Wu, Nano-silver-decorated microfibrous eggshell membrane: processing, cytotoxicity assessment, and optimization, antibacterial activity and wound healing, Sci Rep. 7 (2017) 436.

[2] PH Wang, BS Huang, HC Horng, CC Yeh, YJ Chen, Wound healing, J Chin Med Assoc. 81 (2017).

[3] X Wen, Y Zheng, J Wu, L Yue, C Wang, J Luan, Z Wu, K Wang, In vitro and in vivo investigation of bacterial cellulose dressing containing uniform silver sulfadiazine nanoparticles for burn wound healing, Prog. Nat. Sci.25 (2015) 197-203.

[4] V Planz, J Wang, M Windbergs, Establishment of a cell-based wound healing assay for bio-relevant testing of wound therapeutics, J Pharmacol Toxicol Methods. 89 (2017) 19-25.

[5] TV Tran, THD Phuong, NQ Tran, CK Nguyen, HN Dai, Polymer chitosan-based nanogels as a potential platform for dual targeted drug delivery in cancer therapy, Int. J. Nanotechnol. 15 (2018) 188-189.

[6] J Jin, H Tu, J Chen, G Cheng, X Shi, H Deng, Z Li, Y. Du, Rectorite-intercalated nanoparticles for improving controlled release of doxorubicin hydrochloride, Int J Biol Macromol. 101 (2017) 815-822.

[7] G Lan, B Lu, T Wang, L Wang, J Chen, K Yu, J Liu, F Dai, D Wu, Chitosan/gelatin composite sponge is an absorbable surgical hemostatic agent, Colloids Surf B Biointerfaces. 136 (2015) 1026-34.

[8] N Devi, J Dutta, Preparation and characterization of chitosan-bentonite nanocomposite films for wound healing application, Int. J. Biol. Macromol. 104 (2013) 1897-904.

[9] W Huang, X Li, Y Xue, R Huang, H Deng, Z Ma, Antibacterial multilayer films fabricated by LBL immobilizing lysozyme and HTCC on nanofibrous mats, Int J Biol Macromol. 53 (2013) 26-31.

[10] X Li, H Tu, M Huang, J Chen, X Shi, H Deng, S Wang, Y Du, Incorporation of lysozyme-rectorite composites into chitosan films for antibacterial properties enhancement, Int J Biol Macromol.102 (2017) 789-795.

[11] J Chen, G Cheng, R Liu, Y Zheng, M Huang, Y Yi, X Shi, Y Du, H Deng, Enhanced physical and biological properties of silk fibroin nanofibers by layer-by-layer deposition of chitosan and rectorite, J Colloid Interface Sci. 523 (2018) 208-216.

[12] D Zhang, H Zhao, Z Fan, M Li, P Du, C Liu, Y Li, H Li, H Cao, A Highly Sensitive and Selective Hydrogen Peroxide Biosensor Based on Gold Nanoparticles and Three-Dimensional Porous Carbonized Chicken Eggshell Membrane. Plos One. 10 (2015) e0130156.

[13] S Park, KS Choi, D Lee, D Kim, KT Lim, KH Lee, H Seonwoo, J Kim, Eggshell membrane: Review and impact on engineering, Biosyst. Eng. 151 (2016) 446-63.

[14] MK Sah, SN Rath, Soluble eggshell membrane: A natural protein to improve the properties of biomaterials used for tissue engineering applications. Mater Sci Eng C Mater Biol Appl. 67 (2016) 807-21.

[15] E Ohto-Fujita, T Konno, M Shimizu, K Ishihara, T Sugitate, J Miyake, K Yoshimura, K Taniwaki, T Sakurai, Y Hasebe, Y Atomi, Hydrolyzed eggshell membrane immobilized on phosphorylcholine polymer supplies extracellular matrix environment for human dermal fibroblasts, Cell Tissue Res. 345 (2011) 177-90.

[16] Y Zadik, Self-treatment of full-thickness traumatic lip laceration with the chicken eggshell membrane, Wilderness Environ Med. 18 (2007) 230-1.
[17] JY Yang, SS Chuang, WG Yang, PK Tsay, Egg membrane as a new biological dressing in split-thickness skin graft donor sites: a preliminary clinical evaluation, Chang Gung Med J. 26 (2003) 153-9.
[18] F Guarderas, Y Leavell, T Sengupta, M Zhukova, TL Megraw, Assessment of Chicken-Egg Membrane as a Dressing for Wound Healing, Adv Skin Wound Care. 29 (2016) 131-4.
[19] H Xie, X Chen, X Shen, Y He, W Chen, Q Luo, W Ge, W Yuan, X Tang, D Hou, D Jiang, Q Wang, Y Liu, Q Liu, K Li, Preparation of Chitosan-collagen-alginate Composite Dressing and Its Promoting Effects on Wound Healing, Int J Biol Macromol. 107 (2017) 93-104.
[20] Y Ma, L Xin, H Tan, M Fan, J Li, Jia Y, Z Ling, Y Chen, X Hu, Chitosan membrane dressings toughened by glycerol to load antibacterial drugs for wound healing, Mater Sci Eng C Mater Biol Appl. 81 (2017) 522-531.
[21] M Rezvanian, N Ahmad, MC Mohd Amin, SF Ng, Optimization, characterization, and in vitro assessment of alginate-pectin ionic cross-linked hydrogel film for wound dressing applications, Int J Biol Macromol. 97 (2017)131-140.
[22] Z Cao, Z Shen, X Luo, H Zhang, Y Liu, N Cai, Y Xue, F Yu, Citrate-modified maghemite enhanced binding of chitosan coating on cellulose porous membranes for potential application as a wound dressing, Carbohydr Polym. 166 (2017) 320-328.
[23] MR Reithofer, A Lakshmanan, AT Ping, JM Chin, CA Hauser, In situ synthesis of size-controlled, stable silver nanoparticles within ultrashort peptide hydrogels and their anti-bacterial properties, Biomaterials. 35 (2014) 7535-42.
[24] J Li, D Zhai, F Lv, Q Yu, H Ma, J Yin, Z Yi, M Liu, J Chang, C Wu, Preparation of copper-containing bioactive glass/eggshell membrane nanocomposites for improving angiogenesis, antibacterial activity and wound healing, Acta Biomater. 36 (2016) 254-66.
[25] N.Y.C Nagai, Effects of Ophthalmic Formulations Containing Cilostazol Nanoparticles on Retinal Vasoconstriction in Rats Injected with Endothelin-1, Eprint Arxiv. 26 (2015) 221-302.
[26] R Toy, PM Peiris, KB Ghaghada, E Karathanasis, Shaping cancer nanomedicine: the effect of particle shape on the in vivo journey of nanoparticles, Nanomedicine (Lond). 9 (2014) 121-34.
[27] KH Matthews, HN Stevens, AD Auffret, MJ Humphrey, Eccleston GM, Formulation, stability and thermal analysis of lyophilized wound healing wafers containing an insoluble MMP-3 inhibitor and a non-ionic surfactant, Int J Pharm. 356 (2008) 110-20.
[28] Y Zheng, S Ji, H Wu, S Tian, Y Zhang, L Wang, H Fang, P Luo, X Wang, X Hu, S Xiao, Z Xia, Topical administration of cryopreserved living micronized amnion accelerates wound healing in diabetic mice by modulating local microenvironment, Biomaterials. 113 (2017) 56-67.
[29] M Lavorgna, F Piscitelli, P Mangiacapra, GG Buonocore, Study of the combined effect of both clay and glycerol plasticizer on the properties of chitosan films, Carbohydr Polym. 82 (2010) 291-8.
[30] S Ifuku, A Ikuta, H Izawa, M Morimoto, H Saimoto, Control of mechanical properties of chitin nanofiber film using glycerol without losing its characteristics, Carbohydr Polym. 101 (2014) 714-7.
[31] L Vinklarkova, R Masteikova, G Foltynova, J Muselik, S Pavlokova, J Bernatoniene, D Vetchy, Film wound dressing with local anesthetic based on insoluble carboxymethylcellulose matrix, J. Appl. Biomed. 15 (2017) 313-320.

449 [32] A Nouri, MT Yaraki, M Ghorbanpour, S Agarwal, VK Gupta, Enhanced Antibacterial effect
450 of chitosan film using Montmorillonite/CuO nanocomposite, Int J Biol Macromol.109 (2017)
451 1219-1231.
452 [33] RS Vieira, MM Beppu, Mercury Ion Recovery Using Natural and Crosslinked Chitosan
453 Membranes. Adsorpt.-J. Int. Adsorpt. Soc. 11 (2005) 731-6.
454 [34] DA Murguía-Flores, J Bonilla-Ríos, MR Canales-Fiscal, A Sánchez-Fernández, Protein
455 adsorption through Chitosan–Alginate membranes for potential applications, Chem Cent J. 10
456 (2016) 26.
457 [35] H Chambi, C Grosso, Edible films produced with gelatin and casein cross-linked with
458 transglutaminase, Food Res Int. 39 (2006) 458-66.
459 [36] S Shankar, JW Rhim, Preparation of sulfur nanoparticle-incorporated antimicrobial chitosan
460 films, Food Hydrocolloids. 39 (2018) 458-466.
461 [37] M Baláž, Eggshell membrane biomaterial as a platform for applications in materials science,
462 Acta Biomater. 10 (2014) 3827-43.
463 [38] K Baysal, AZ Aroguz, Z Adiguzel, BM Baysal, Chitosan/alginate crosslinked hydrogels:
464 preparation, characterization, and application for cell growth purposes, International Journal of
465 Biological Macromolecules. 59 (2013) 342-8.
466 [39] H Hajiali, M Summa, D Russo, A Armirotti, V Brunetti, R Bertorelli, A Athanassiou, E Mele,
467 Alginate–lavender nanofibers with antibacterial and anti-inflammatory activity to effectively
468 promote burn healing, J. Mat. Chem. B. 4 (2016) 1686-95.
469 [40] T Yan, F Cheng, X Wei, Y Huang, J He, Biodegradable collagen sponge reinforced with
470 chitosan/calcium pyrophosphate nanoflowers for rapid hemostasis, Carbohydr Polym. 170 (2017)
471 271-280.
472 [41] SH Wang, Y Jing, Study on the barrier properties of glycerol to chitosan coating layer, Mater
473 Lett. 209 (2017) 345-348.
474 [42] FH Xu, BC Weng, LA Materon, R Gilkerson, K Lozano, Large-scale production of aternary
475 composite nanofiber membrane for wound dressing applications, J Bioact Compat Polym. 29
476 (2014) 646-660.
477 [43] FH Xu, BC Weng, R Gilkerson, LA Materon, K Lozano, Development of tannic
478 acid/chitosan/pullulan composite nanofibers from aqueous solution for potential applications as
479 wound dressing, Carbohydr Polym. 115 (2015) 16-24.
480 [44] O Castaño, S Pérez-Amodio, C Navarro-Requena, MÁ Mateos-Timoneda, Engel E4
481 Instructive microenvironments in skin wound healing: Biomaterials as signal releasing platforms,
482 Adv Drug Deliv Rev. 129 (2018) 95-117.
483 [45] CR Kruse, M Singh, S Targosinski, I Sinha, JA Sørensen, E Eriksson, K Nuutila, The effect
484 of pH on cell viability, cell migration, cell proliferation, wound closure and wound
485 re-epithelialization: in vitro and in vivo study, Wound Repair Regen. 25 (2017) 260-269.
486 [46] MSM Eldin, EA Soliman, AI Hashem, TM Tamer, Chitosan modified membranes for wound
487 dressing applications: preparations, characterization and bio-evaluation, Trends in Biomaterials &
488 Artificial Organs. 22 (2009) 158-68.
489 [47] PB Kandagal, S Ashoka, J Seetharamappa, SM Shaikh, Y Jadegoud, OB Ijare, Study of the
490 interaction of an anticancer drug with human and bovine serum albumin: spectroscopic approach.
491 J Pharm Biomed Anal. 41 (2006) 393-9.
492 [48] G Li, J Huang, T Chen, X Wang, H Zhang, Q Chen, Insight into the interaction between

chitosan and bovine serum albumin, Carbohydr Polym. 176 (2017) 75-82.
[49] R Qi, X Cao, M Shen, R Guo, J Yu, X Shi, Biocompatibility of Electrospun Halloysite Nanotube-Doped Poly(Lactic-co-Glycolic Acid) Composite Nanofibers, J Biomater Sci Polym Ed. 23 (2012) 299-313.

Captions

Tables

Table 1: Proportion of CS, ESM powder and glycerol in the prepared blend films.

Table 2: Morphological characterization of CS and blend films in terms of thickness and mass.

Figures

Figure 1: Particle size distribution of ESM powder.

Figure 2: Appearance and transparency of chitosan (CS) and blend films with varying ratios of glycerol (v/v, %) and ESM powder (w/v, g/mL).

Figure 3: Scanning electron microscopy images of CS (a) and blend (b-e) films. (b) 1G-0.01ESM/CS film at 100x magnification; (c) 2G-0.01ESM/CS film at 100x magnification; (d) 1G-0.02ESM/CS film at 100x magnification; (e) 2G-0.02ESM/CS film at 100x magnification.

Figure 4: Degradation rate of CS (1) and ESM/CS blend (2-5) films in lysozyme/PBS solution. (a) The CS and blend films were immersed in 1 mg/mL lysozyme/PBS for different time (1, 2 and 3 days). 1: CS film; 2: 1G-0.01 ESM/CS film; 3: 2G-0.01ESM/CS film; 4: 1G-0.02ESM/CS film; 5: 2G-0.02ESM/CS film.

Figure 5: Dressing pH of CS and blend films.

Figure 6: The wound fluid absorption rate (A) and absorptive capacity (B) of BSA of CS and blend films.

Figure 7: Graphical representation of OD measurements in *Escherichia coli* (A) and *Staphylococcus aureus* (B) after 24 h incubation.

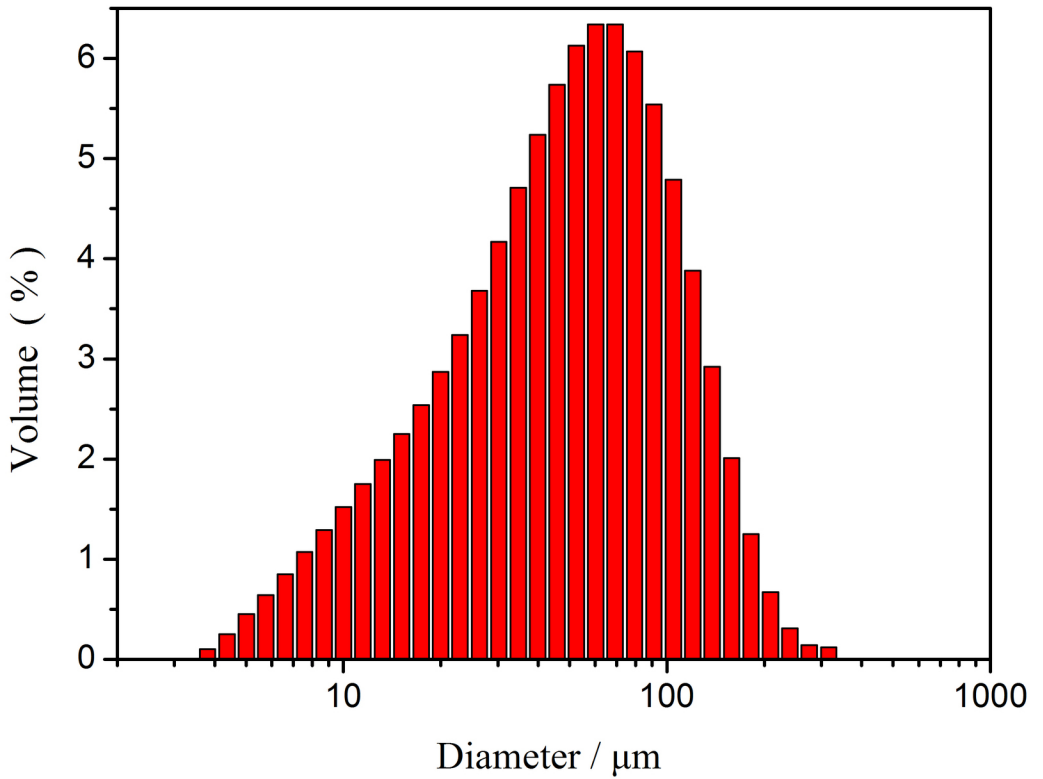
Volume (%)
0
1
2
3
4
5
6
10
100
1000
Diameter / μm

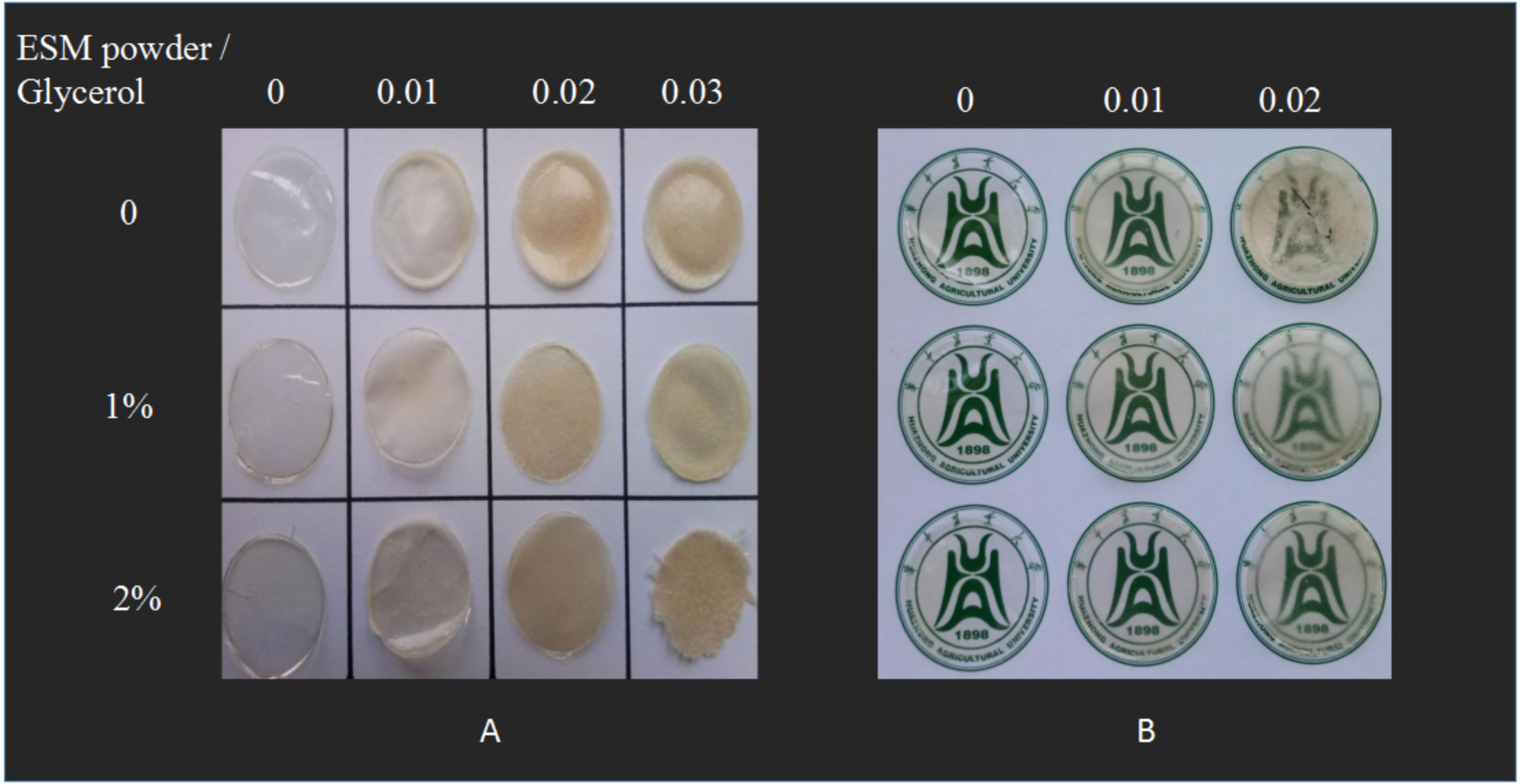
ESM powder /
Glycerol
0
0.01
0.02
0.03
0
1%
2%
A
0
0.01
0.02
B

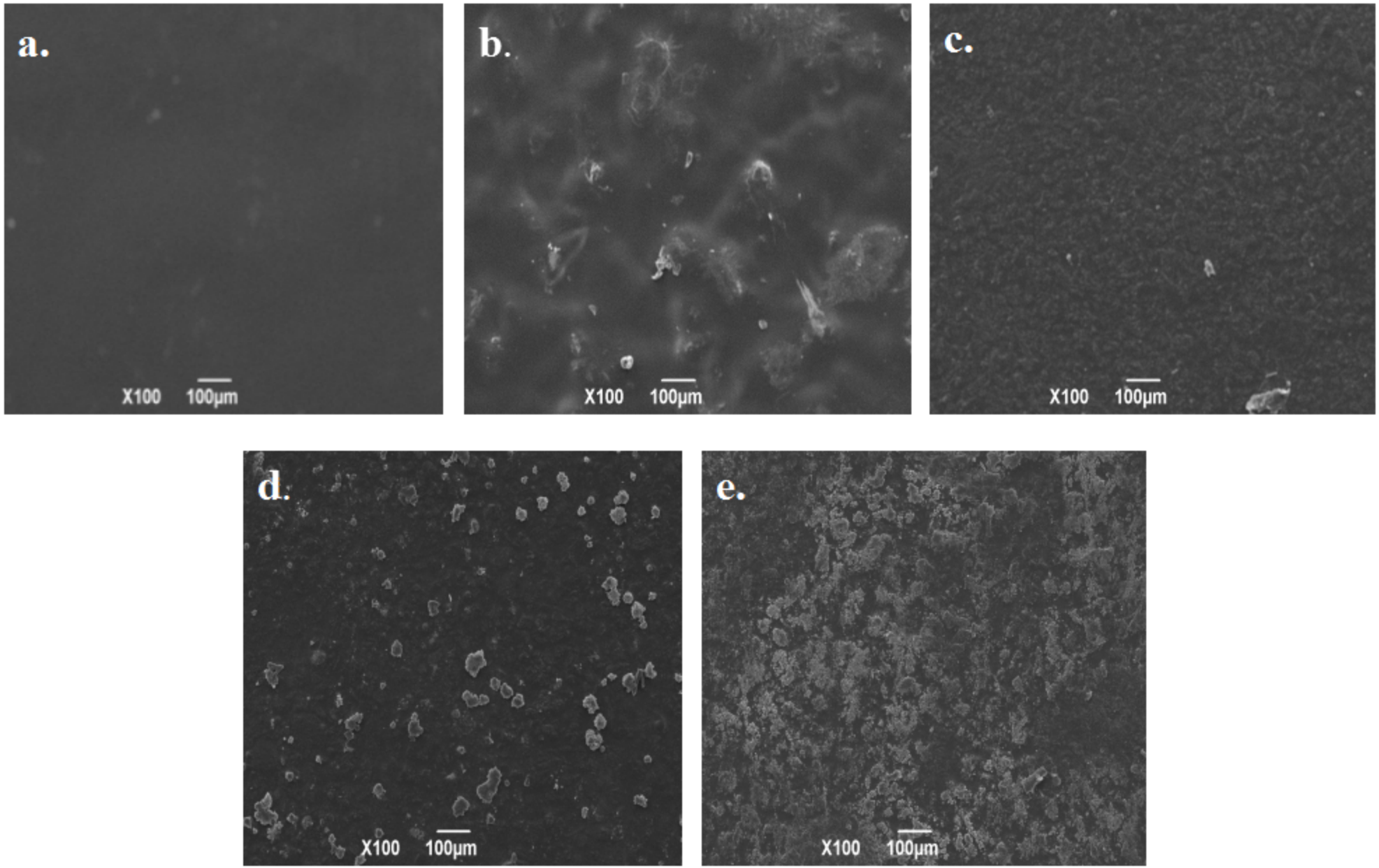
a.
X100 100µm
b.
X100 100µm
c.
X100 100µm
d.
X100 100µm
e.
X100 100µm

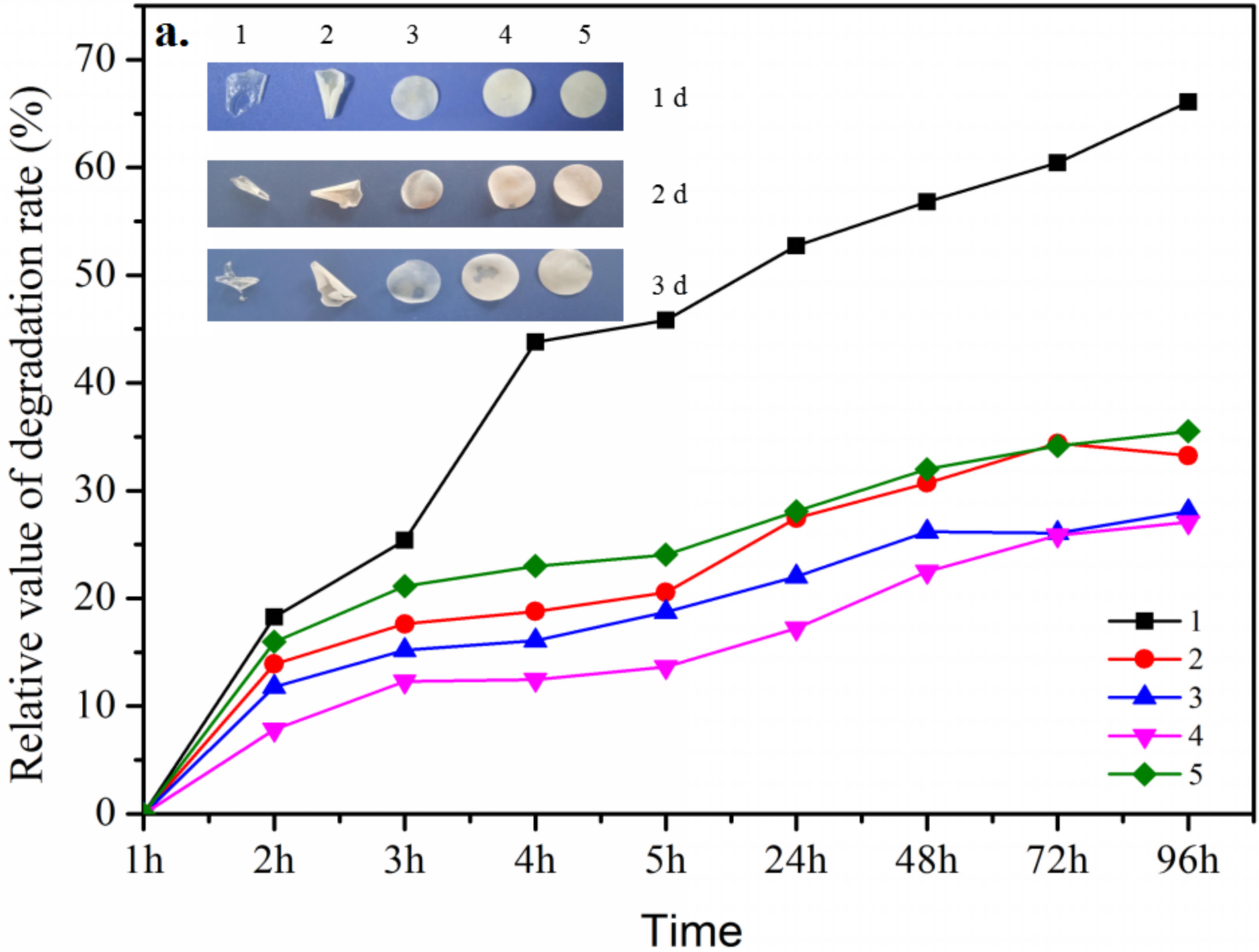
a.
1
2
3
4
5
1 d
2 d
3 d
Relative value of degradation rate (%)
0
10
20
30
40
50
60
70
1h
2h
3h
4h
5h
24h
48h
72h
96h
Time
1
2
3
4
5

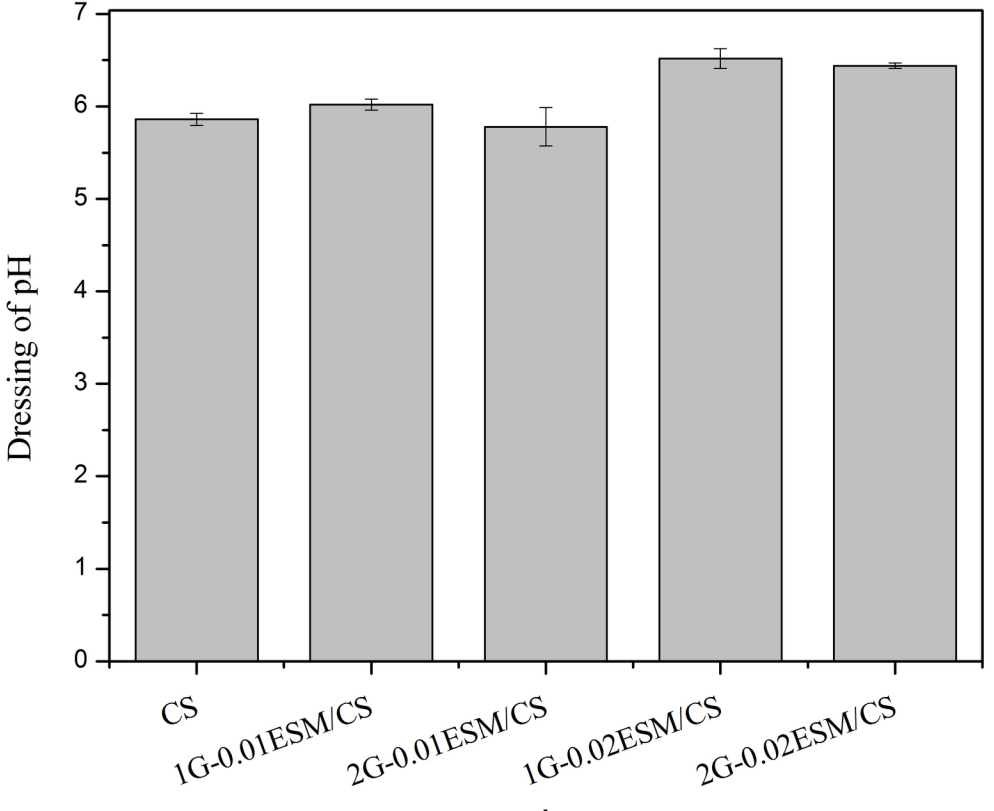
Dressing of pH
0
1
2
3
4
5
6
7
CS
1G-0.01ESM/CS
2G-0.01ESM/CS
1G-0.02ESM/CS
2G-0.02ESM/CS

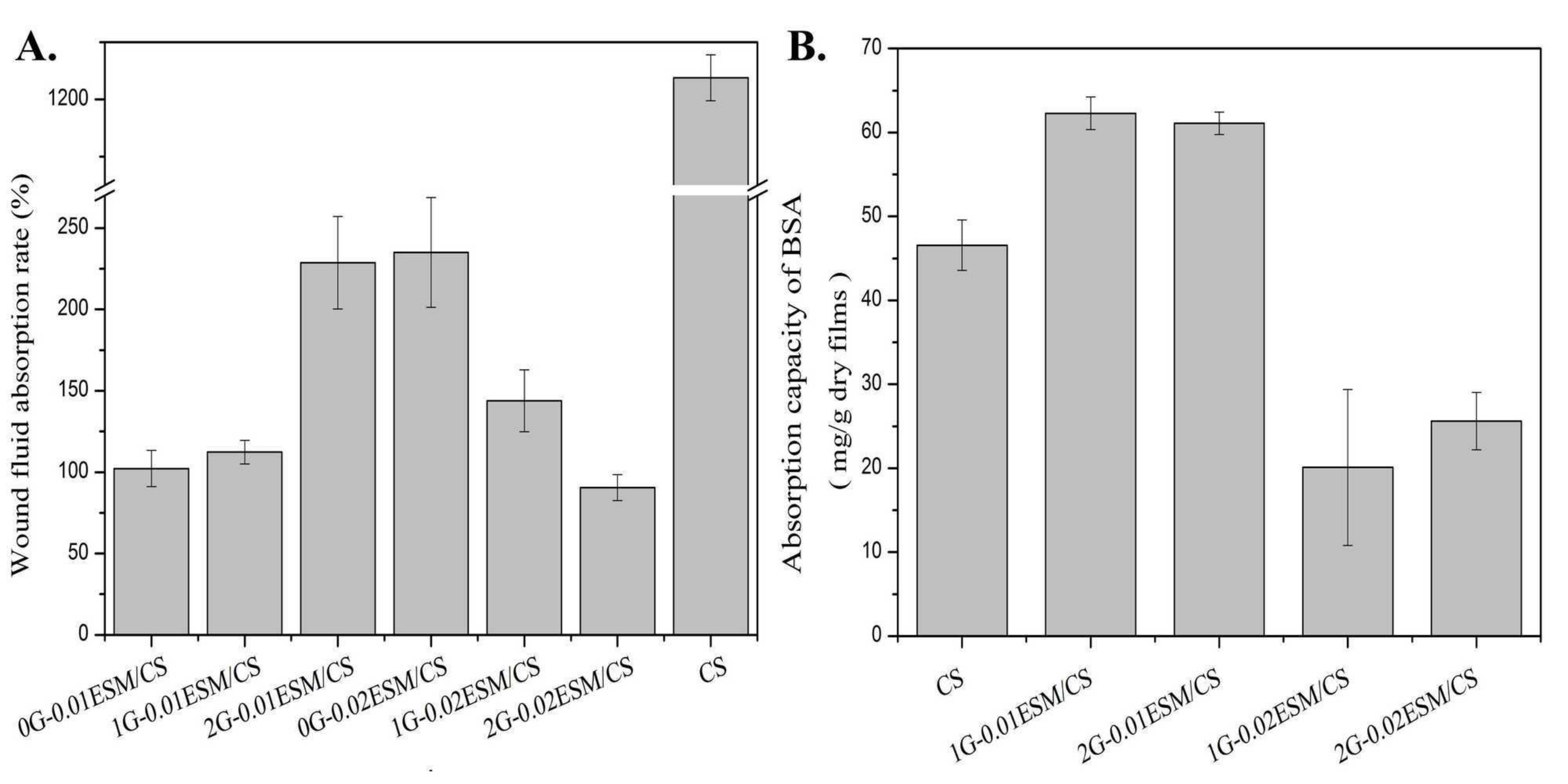
A.
Wound fluid absorption rate (%)
1200
250
200
150
100
50
0
0G-0.01ESM/CS
1G-0.01ESM/CS
2G-0.01ESM/CS
0G-0.02ESM/CS
1G-0.02ESM/CS
2G-0.02ESM/CS
CS
B.
Absorption capacity of BSA
(mg/g dry films)
70
60
50
40
30
20
10
0
CS
1G-0.01ESM/CS
2G-0.01ESM/CS
1G-0.02ESM/CS
2G-0.02ESM/CS

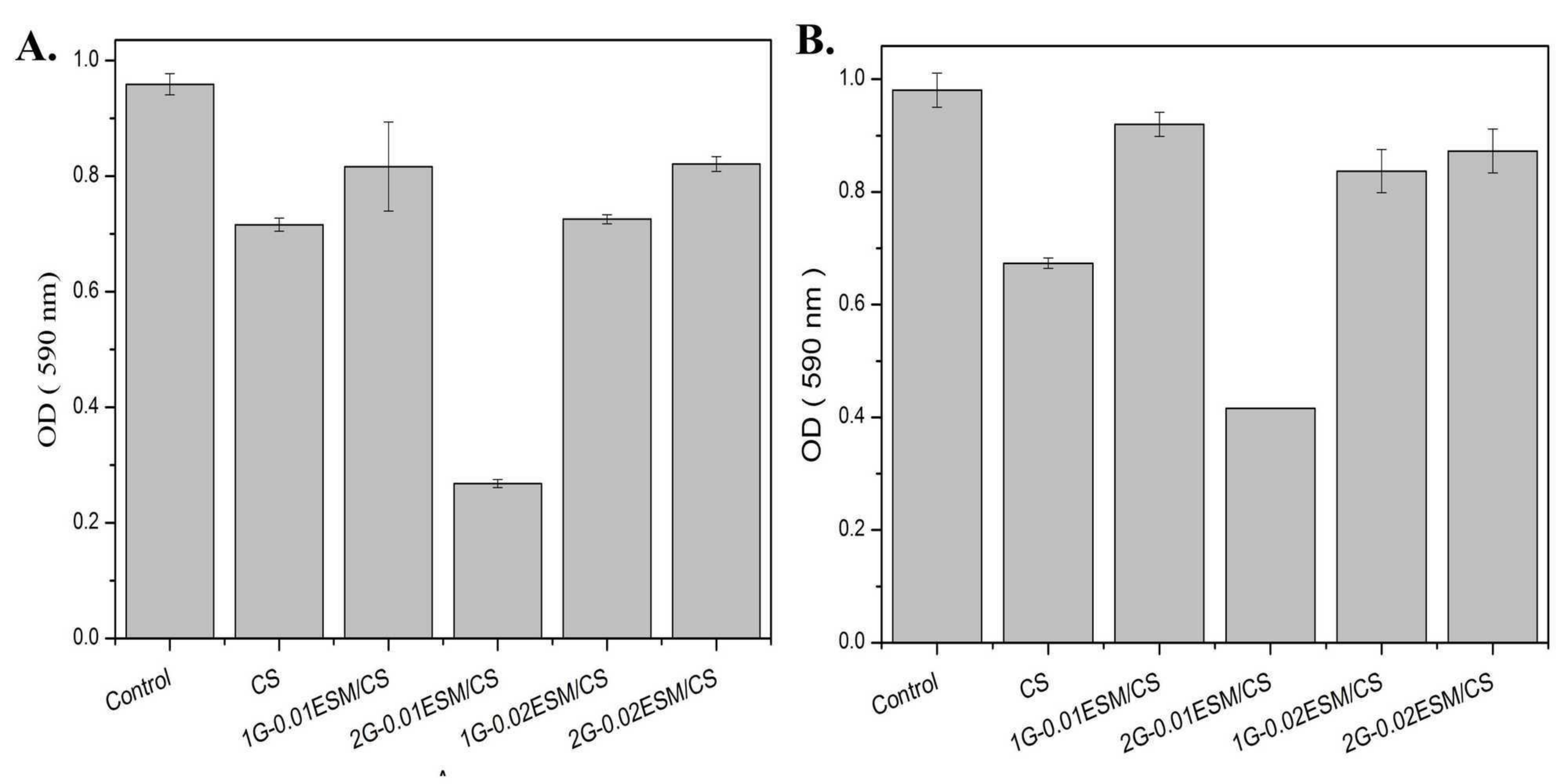
A.
OD (590 nm)
1.0
0.8
0.6
0.4
0.2
0.0
Control
CS
1G-0.01ESM/CS
2G-0.01ESM/CS
1G-0.02ESM/CS
2G-0.02ESM/CS
B.
OD (590 nm)
1.0
0.8
0.6
0.4
0.2
0.0
Control
CS
1G-0.01ESM/CS
2G-0.01ESM/CS
1G-0.02ESM/CS
2G-0.02ESM/CS

S.No.	Sample code	Glycerol (%)	ESM powder (g/mL)
1	CS	0	0
2	1G-0ESM/CS	1	0
3	2G-0ESM/CS	2	0
4	0G-0.01ESM/CS	0	0.01
5	1G-0.01ESM/CS	1	0.01
6	2G-0.01ESM/CS	2	0.01
7	0G-0.02ESM/CS	0	0.02
8	1G-0.02ESM/CS	1	0.02
9	2G-0.02ESM/CS	2	0.02
10	0G-0.03ESM/CS	0	0.03
11	1G-0.03ESM/CS	1	0.03
12	2G-0.03ESM/CS	2	0.03

Sample code	Mass of different position of the same film (mg)	Mass of the same position of different film (mg)	Thickness (mm)
1G-0.01ESM/CS	2.73 ± 0.06	11.8 ± 0.53	0.17 ± 0.07
2G-0.01ESM/CS	2.3 ± 0.21	13.3 ± 0.10	0.24 ± 0.03
1G-0.02ESM/CS	3.4 ± 0.20	15.33 ± 1.07	0.19 ± 1.00
2G-0.02ESM/CS	3.37 ± 0.23	14.47 ± 0.97	0.23 ± 0.02